

Formal encapsulation of $[\text{Fe}(\text{H}_2\text{O})_6]^{3+}$ by $\{\text{Fe}_2(\text{hppta})\}$ units gives a system of $S = 13/2$ Fe^{III}_9 oxo clusters showing magnetic hysteresis

Wolfgang Schmitt,^{a,b} Christopher E. Anson,^a Wolfgang Wernsdorfer^c and Annie K. Powell*^a

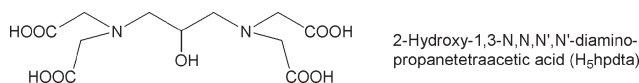
Received (in Cambridge, UK) 4th November 2004, Accepted 8th February 2005

First published as an Advance Article on the web 4th March 2005

DOI: 10.1039/b416766j

Under solvothermal conditions the unprecedented nonanuclear Fe^{III} aggregate $[\text{Fe}_9(\mu_3\text{-O})_4(\mu\text{-OH})_4(\text{hppta})_4]^{5-}$ is formed through the formal encapsulation of $[\text{Fe}(\text{H}_2\text{O})_6]^{3+}$ by four $[\text{Fe}_2(\text{hppta})(\text{H}_2\text{O})_2]^+$ units: the aggregates have ground state spins of $S = 13/2$ while the observed hysteresis below 1.8 K results from inter-cluster antiferromagnetic coupling.

The synthesis and structures of polynuclear Fe^{III} -oxo-complexes have been investigated intensively to provide model compounds of biological systems and to elucidate mechanisms of biomineratisation processes.^{1,2} In recent years interest in this class of compounds has also increased due to their potential applications with particular focus on their magnetic properties.³ The objective of numerous research groups is the optimisation of their synthetic strategies to prepare clusters with dimensions ranging between simple paramagnets and infinite solid-state structures displaying superparamagnetic behaviour.^{4,5} Although a rationalised build-up of polynuclear iron compounds is currently still more a wish than a reality, the structures of compounds resulting from a systematic synthetic programme provide useful pointers to the parameters influencing cluster formation. This is one approach, and the one we favour, to the isolation of cluster species and requires identification of persistent structural motifs which can to some extent direct the serendipitous assembly process.^{6,7}



Previously we have investigated the homologous build-up of oxo/hydroxo-clusters with the dinucleating ligand H_5hppta . $[\text{Fe}_2(\text{hppta})(\text{H}_2\text{O})_2]^+$ building units (formed *in situ*, but which can be trapped as the neutral chloride adduct $[\text{Fe}_2(\text{hppta})\text{Cl}(\text{H}_2\text{O})_3]$) were linked *via* hydrolytic condensation reactions with loss of both H^+ and water ligands. In this context we previously reported the structures and magnetic properties of $[\text{Fe}_2(\text{hppta})\text{Cl}(\text{H}_2\text{O})_3]$, the tetranuclear Fe^{III} species $[\text{Fe}_4(\mu\text{-O})(\mu\text{-OH})(\text{hppta})_2(\text{H}_2\text{O})_4]^-$ which has a planar rectangular arrangement of the metal ions, the hexanuclear aggregate $[\text{Fe}_6(\mu\text{-O})(\mu\text{-OH})_5(\text{hppta})_3]^{4-}$ in which a dinuclear unit has capped the rectangular Fe_4 -plane.⁷ Besides these aggregation processes we also initiated core rearrangements reactions where the square planar complex transforms into a complex $[\text{Fe}_4(\mu\text{-O})(\mu\text{-OH})_4(\text{hppta})_2]^{3-}$ with a tetrahedral structure of the metal ions depending on the pH in the reaction system.

We have also shown how M^{III} /ligand shells ($\text{M} = \text{Fe}, \text{Al}$) can effectively encapsulate fragments of M^{III} hydroxide minerals.⁸⁻¹⁰

*powell@chemie.uni-karlsruhe.de

In the specific case of the H_5hppta system, dinuclear $\{\text{M}_2(\text{hppta})(\text{H}_2\text{O})_4\}^+$ units can encapsulate mineral fragments or small inorganic cationic hydroxo complexes to form larger aggregates. The dodecanuclear Fe^{III} complex $[\{\text{Fe}_6(\mu_3\text{-O})_2(\mu\text{-OH})_2(\text{hppta})_2(\text{H}_4\text{hppta})_2\}_2]$ is a dimer of a hexanuclear unit, in which two $\{\text{Fe}_2\text{hppta}\}$ units have trapped a dinuclear $[(\text{H}_2\text{O})_4\text{Fe}(\mu\text{-OH})_2\text{Fe}(\text{H}_2\text{O})_4]^{4+}$ complex,⁷ while the aluminium aggregate $[\text{Al}_{15}(\mu_3\text{-O})_4(\mu_3\text{-OH})_6(\mu\text{-OH})_{14}(\text{hppta})_4]^{3-}$ results from the condensation of four $[\text{Al}_2(\text{hppta})(\text{H}_2\text{O})_4]^+$ units with an Al_7 -boehmite-type mineral fragment $[\text{Al}_7(\text{OH})_{12}(\text{H}_2\text{O})_{12}]^{9+}$.⁸

Here we report the synthesis, structure and magnetic properties of a nonanuclear aggregate $[\text{Fe}_9(\mu_3\text{-O})_4(\mu\text{-OH})_4(\text{hppta})_4]^{5-}$ (**1**) in which a central Fe^{III} ion is surrounded by four dinuclear $\{\text{Fe}_2\text{hppta}\}$ units (Fig. 1).

Reaction of $\text{Fe}(\text{NO}_3)_3 \cdot 9\text{H}_2\text{O}$ (0.604 g, 1.5 mmol), H_5hppta (0.081 g, 0.25 mmol) and KHCO_3 (0.12 g) in MeOH (8 ml) at 120 °C in a Teflon-lined autoclave for 15 h, followed by slow cooling, yields principally haematite along with brown cubic crystals† of $\text{K}_5[\text{Fe}_9(\mu_3\text{-O})_4(\mu\text{-OH})_4(\text{hppta})_4] \cdot 5\text{H}_2\text{O} \cdot 5\text{CH}_3\text{OH}$ ($\text{K}_5\text{[I]} \cdot 5\text{H}_2\text{O} \cdot 5\text{CH}_3\text{OH}$) in 10–20% yield (based on ligand) with satisfactory CHN analysis. Although this is the minor product, the synthesis is completely reproducible and the product can be separated mechanically (hence the range of yields), with no evidence of the iron oxide impurities as established from X-ray powder patterns and the variable field magnetic susceptibility measurements. The alternative route using the preformed dinuclear units and the hexaaqua ion directly also leads to the compound but is not such a clean synthetic route with a number of side-products.

Fig. 2 illustrates the $[\text{Fe}_9(\mu_3\text{-O})_4(\mu\text{-OH})_4(\text{hppta})_4]^{5-}$ aggregate **1** and its $\text{Fe}-\text{O}$ core. The central Fe^{III} , $\text{Fe}(1)$, located on an inversion centre, is connected to six further Fe^{III} centres ($\text{Fe}(2)$, $\text{Fe}(3)$, $\text{Fe}(4)$ and symmetry equivalents) *via* four μ_3 -oxides ($\text{O}(1)$, $\text{O}(2)$, $\text{O}(1')$ and $\text{O}(2')$) in an essentially planar arrangement. There are two

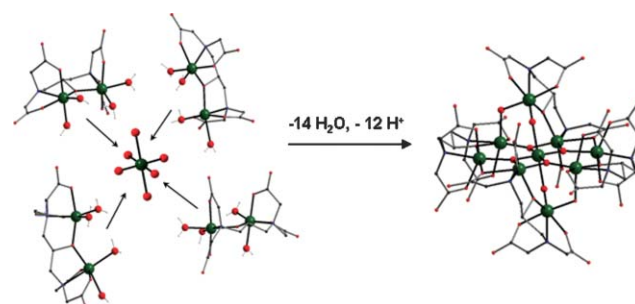


Fig. 1 Formal hydrolytic encapsulation of $[\text{Fe}(\text{H}_2\text{O})_6]^{3+}$ by four $\{\text{Fe}_2(\text{hppta})(\text{H}_2\text{O})_4\}^+$ species to give $[\text{Fe}_9(\mu_3\text{-O})_4(\mu\text{-OH})_4(\text{hppta})_4]^{5-}$.

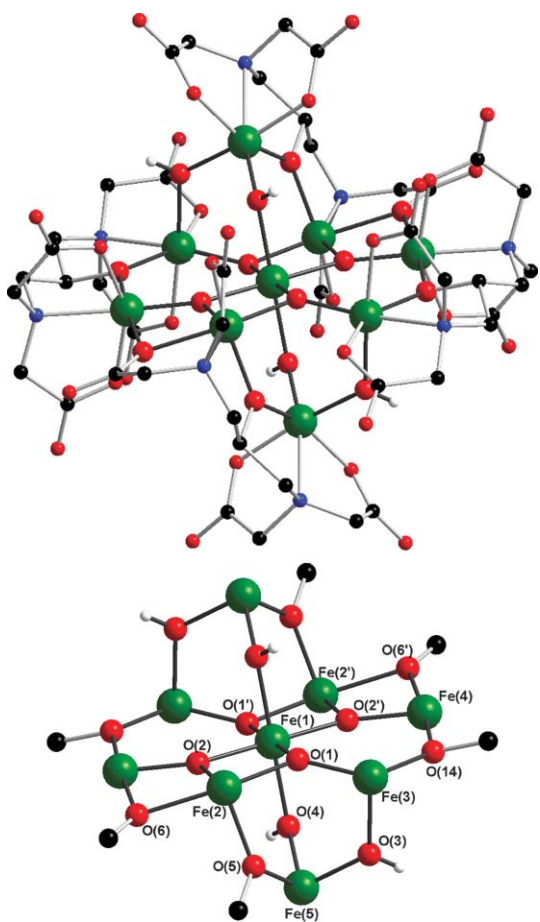


Fig. 2 Structure of the Fe_9 aggregate **1** in $\text{K}_5[\mathbf{1}]\cdot 5\text{MeOH}\cdot 5\text{H}_2\text{O}$ (above) and the aggregate core (below). Colour code: Fe, green; O, red; N, blue; C, black; H, white. $\text{Fe}-\langle\mu_3\text{-O}\rangle$ 1.837(3)–2.013(3) Å, $\text{Fe}-\langle\mu\text{-O}\rangle$ 1.938(4)–2.083(4) Å. Angles at O (°): $\text{Fe}(1)\text{-O}(1)\text{-Fe}(2)$ 96.0(1), $\text{Fe}(1)\text{-O}(1)\text{-Fe}(3)$ 129.2(2), $\text{Fe}(2)\text{-O}(1)\text{-Fe}(3)$ 128.8(2), $\text{Fe}(1)\text{-O}(2)\text{-Fe}(2)$ 97.4(1), $\text{Fe}(1)\text{-O}(2)\text{-Fe}(4')$ 150.4(2), $\text{Fe}(2)\text{-O}(1)\text{-Fe}(4')$ 112.2(2), $\text{Fe}(3)\text{-O}(3)\text{-Fe}(5)$ 123.8(2), $\text{Fe}(1)\text{-O}(4)\text{-Fe}(5)$ 124.5(2), $\text{Fe}(2)\text{-O}(5)\text{-Fe}(5)$ 120.2(2), $\text{Fe}(2)\text{-O}(6)\text{-Fe}(4')$ 95.0(1), $\text{Fe}(3)\text{-O}(14)\text{-Fe}(4)$ 128.5(2).

further inversion-related Fe^{III} atoms, $\text{Fe}(5)$ and $\text{Fe}(5')$, located above and below the $\{\text{Fe}_7\text{O}_4\}$ plane. $\text{Fe}(5)$ is situated over the triangular $\text{Fe}(1)\text{/Fe}(2)\text{/Fe}(3)\text{/O}(1)$ moiety and connected to it by one alkoxo-bridge, $\text{Fe}(2)\text{-O}(6)\text{-Fe}(5)$, and two hydroxo-groups, $\text{Fe}(1)\text{-O}(4)\text{-Fe}(5)$ and $\text{Fe}(3)\text{-O}(3)\text{-Fe}(5)$. The oxygen bridging in the core is completed by a second alkoxo bridge, $\text{O}(14)$, and a carboxylate oxygen, $\text{O}(6)$. All nine Fe^{III} atoms in **1** have distorted octahedral coordination environments. The nonanuclear complex is completed by the four fully deprotonated hpdta⁵⁻ ligands binding to pairs of Fe^{III} atoms { $\text{Fe}(2)$ and $\text{Fe}(5)$ } and { $\text{Fe}(3)$ and $\text{Fe}(4')$ } and symmetry equivalents.

The geometry around the central $\text{Fe}(1)$ is slightly distorted octahedral arising from the, not unexpectedly, longer $\text{Fe}(1)\text{-O}(5)_{\text{hydroxo}}$ distance of 2.083(4) Å, compared with the $\text{Fe}(1)\text{-O}_{\text{oxo}}$ lengths of 2.013(3) Å and 1.966(3) Å to $\text{O}(1)$ and $\text{O}(2)$. The $\text{O}(5)\text{-Fe}(1)\text{-O}(5')$ angle is constrained to be 180° by symmetry, but the angles within the square plane, whilst totalling 360° are markedly different with $\text{O}(1)\text{-Fe}(1)\text{-O}(2)$ at 98° and $\text{O}(1)\text{-Fe}(1)\text{-O}(2')$ at 82°. This distortion is likely to result from the electrostatic repulsion between $\text{Fe}(1)$ and $\text{Fe}(2)$ and $\text{Fe}(1)$ and $\text{Fe}(2')$ which are part of

three edge-sharing octahedra with $\text{O}(1)$ and $\text{O}(2')$ and $\text{O}(1')$ and $\text{O}(2)$ as the common edges. Overall, whilst the μ_3 -oxides have essentially planar environments there are significant deviations from the idealised 120° angles.

The core in **1** can be seen as the formal encapsulation of an $[\text{Fe}(\text{H}_2\text{O})_6]^{3+}$ -ion by condensation with four $[\text{Fe}_2(\text{hpdta})(\text{H}_2\text{O})_4]^+$ -units with the concomitant loss of 14 water molecules and 12 protons (Fig. 1). Ferric nitrate, the starting material, in addition to contributing nine equivalents of water per Fe^{III} is a rare example of an Fe^{III} compound containing the hexaaqua ion¹¹ which, whilst widely postulated, is hardly ever directly observed due to the ready hydrolysis initiated by the high spin Fe^{III} ion in protic media.¹² The observed coordination geometry around $\text{Fe}(1)$ together with the facts that we have previously observed the trapping of the higher homologues of such hydrolysis reactions^{6–10} and that we can use complexes containing { Fe_2hpdta } units as starting materials for the synthesis of **1** lends support to the idea that a mononuclear Fe^{III} species derived from $[\text{Fe}(\text{H}_2\text{O})_6]^{3+}$ is encapsulated during the synthesis.

The structure of **1** is consistent with the results of our previous studies of $\text{M}^{\text{III}}/\text{hpdta}$ complexes.^{7,8} These clearly demonstrate that the hpdta⁵⁻ ligand always ligates two Fe^{III} ions in a similar, predictable coordination mode, leaving two *cis*-related vacant coordination sites on each octahedral metal centre which are either occupied by terminal (*e.g.*, H_2O) or bridging (OH^- or O^{2-}) ligands. In aqueous, ambient reaction systems, aggregation to larger clusters occurs through deprotonation and condensation reactions involving the terminal water ligands; the geometric restrictions imposed by the hpdta⁵⁻ ligand then leads to oligonuclear Fe^{III} aggregates with mostly predictable structures.⁶ Although the formation of **1** could easily be rationalised on the basis of these earlier studies, it is difficult to propose a detailed mechanism under, in this case, solvothermal conditions.

The Fe_9 aggregates pack forming a lattice that can conveniently be described as a distorted trigonally-compressed primitive-cubic array, with the unit cell parameters a , b and c of similar length and α , β and γ all obtuse and similar. Assemblages of the K^+ cations serve to link the aggregates into chains parallel to the c axis. In the other two dimensions the aggregates are linked by hydrogen bonding, which is either direct, *e.g.*, the hydroxo ligand $\text{O}(3)\text{-H}(3)$ forms a hydrogen bond to the carboxylate oxygen $\text{O}(11)$ or indirect, *via* the methanol and water molecules in the lattice.

The temperature dependence of the magnetic susceptibility of $\text{K}_5[\mathbf{1}]\cdot 5\text{H}_2\text{O}\cdot 5\text{CH}_3\text{OH}$ was measured between 250 and 1.8 K (Fig. 3). The χT -value of 11.5 emu K mol⁻¹ at 250 K is significantly lower than that expected for nine uncoupled Fe^{III} high-spin ions (39.375 emu mol⁻¹ K with $g = 2$) indicating a range of antiferromagnetic pairwise interactions that give rise to an uncompensated magnetic moment. On lowering the temperature, χT continuously increases up to a maximum of *ca.* 23 emu K mol⁻¹ at 20–14 K followed by a rapid decrease. Such a decrease can be explained by assuming the presence of inter-cluster interactions and/or zero field splitting of the S ground state due to magnetic anisotropy. The temperature dependence of the susceptibility below 14 K can reasonably be approximated to a Curie–Weiss behaviour with $C = Ng^2\mu_{\text{B}}^2/3k_{\text{B}} S(S + 1) = 25.0$ emu K mol⁻¹ which is not far from the value expected for $S = 13/2$ (24.4 emu K mol⁻¹ with $g = 2$), and a negative Weiss temperature $\theta = -1.2$ K, indicative of weak antiferromagnetic

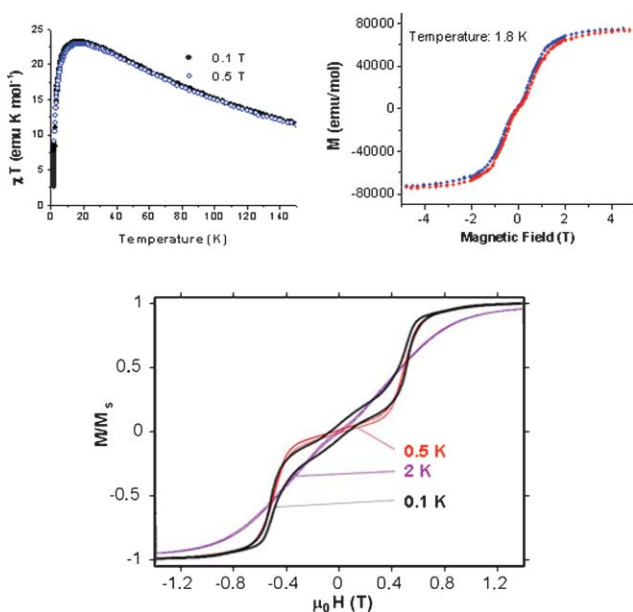


Fig. 3 Magnetic properties of $\text{K}_5[\mathbf{1}] \cdot 5\text{H}_2\text{O} \cdot 5\text{CH}_3\text{OH}$; γT vs. T (top, left), field dependence of the magnetisation at 1.8 K (top, right), μ -SQUID measurements on a single crystal at 2 K, 0.5 K and 0.1 K (below).

inter-cluster interactions. The field dependence of the magnetisation measured at 1.8 K (Fig. 3) reveals a saturation value of *ca.* 74 000 emu mol⁻¹ at 5 T, confirming the calculated spin ground state of $S = 13/2$. The measurement also reveals weak magnetic hysteresis effects.

Micro-SQUID measurements (Fig. 3) at lower temperatures confirm the hysteresis behaviour of $\text{K}_5[\mathbf{1}] \cdot 5\text{H}_2\text{O} \cdot 5\text{CH}_3\text{OH}$ and show an increased coercitivity. No dependence of the hysteresis on sweep rate was observed below *ca.* 0.1 K, indicating that tunnelling is quenched by inter-cluster coupling. At all temperatures studied, a decrease of the slope of the magnetisation around $H = 0$ is evident, which is consistent with the presence of inter-cluster interactions. The “double-S” loops in the hysteresis and the negative Weiss constant both show this coupling to be anti-ferromagnetic. An estimate of the mean intermolecular exchange coupling J_{inter} can be made using $-JS^2 = gS\mu_B H_c$,¹³ where H_c ($= 0.51$ T) is the inflection point of the magnetisation curve (Fig. 3). For $S = 13/2$, $g = 2.0$ this gives $J = -0.11$ K. In addition, further microSQUID measurements at different angles of the applied field show that D is negative, and larger than -0.15 K.

Simplistic spin models leading to a ground state spin of $S = 15/2$ can be envisaged and the deviation of the observed $S = 13/2$ ground spin state from this could be a result of intercluster interactions, perhaps in combination with the ZFS contributions. However, in spite of the observed hysteresis and negative value for D , this system cannot be described in terms of an exchange-biased single molecule magnet (SMM) for the following reasons. For a quantum system like a SMM, the tunnel rate starts to dominate at low temperature and this is reflected by the sweep rate dependence (which becomes temperature independent below the crossover temperature T_c , but does not go to zero). The fact that we observe no sweep rate dependence of the tunnel rate at low temperature means that this molecular (and thus quantum) SMM phenomenon has been quenched, here by the presence of 2-D or 3-D magnetic

ordering within the *quasi-primitive* cubic array of aggregates. The question of whether isolated Fe_9 aggregates would show SMM behaviour must therefore remain open. The magnetic properties of this system will be further studied, for example, by using high field EPR measurements to confirm the D parameter and spin state.

In summary, using solvothermal synthetic methods we have isolated and characterised a system composed of novel nona-nuclear Fe^{III} clusters with $S = 13/2$ ground state spins and displaying hysteresis. The structure of the aggregate is consistent with previously established reactivity patterns for the $\text{Fe}^{\text{III}}/\text{hppta}^{5-}$ system, in which $\{\text{Fe}(\text{hppta})(\text{H}_2\text{O})_4\}^+$ building blocks undergo hydrolytic condensation reactions with themselves as well as with small inorganic cationic fragments.

This work was supported by the DFG (CFN and SPP 1137) and the Special Coordination Funds for Promoting Science and Technology from MEXT, Japan *via* an ICYS Fellowships (to WS).

Wolfgang Schmitt,^{a,b} Christopher E. Anson,^a Wolfgang Wernsdorfer^c and Annie K. Powell^{a*}

^aInstitut für Anorganische Chemie, Universität Karlsruhe, Engesserstr. 15, 76128 Karlsruhe, Germany. E-mail: powell@chemie.uni-karlsruhe.de

^bNational Institute for Materials Science, ICYS, Tsukuba, 1-1 Namiki, Ibaraki 305 0044, Japan

^cLaboratoire Louis Néel, CNRS BP 166, 38042 Grenoble Cedex 9, France

Notes and references

† Crystal details for $\text{K}_5[\mathbf{1}] \cdot 5\text{H}_2\text{O} \cdot 5\text{CH}_3\text{OH}$: $\text{C}_{49}\text{H}_{86}\text{Fe}_9\text{K}_5\text{N}_8\text{O}_{54}$, $M = 2349.41$ g mol⁻¹, orange-brown cube $0.08 \times 0.10 \times 0.10$ mm, triclinic, $P-1$, $a = 12.9507(15)$, $b = 13.7625(17)$, $c = 13.7737(16)$ Å, $\alpha = 105.880(9)^\circ$, $\beta = 113.106(9)^\circ$, $\gamma = 102.777(9)^\circ$, $V = 2016.5(4)$ Å³, $Z = 1$, 200 K, $D_c = 1.935$ Mg m⁻³, $\mu(\text{Mo-K}\alpha) = 1.943$ mm⁻¹, $2\theta_{\text{max}} = 54.4^\circ$, 15893 data, 8248 unique ($R_{\text{int}} = 0.0437$); 672 parameters and 16 restraints, $wR_2 = 0.1648$, $S = 1.040$ (all data), $R_1 = 0.0605$ (6151 with $F \geq 4\sigma(F)$). The K^+ cations and solvent molecules are disordered, and were refined as two assemblages (each with half occupancy) with appropriate K–O geometries, one containing two, the other three K^+ . Crystallographic data (excluding structure factors) have been deposited with CCDC 255071. See <http://www.rsc.org/suppdata/cc/b4/b416766j/> for crystallographic data in .cif or other electronic format.

- 1 Metal Ions in Biological Systems. Iron Transport and Storage in Microorganisms, Plants and Animals, ed. A. Sigel and H. Sigel, Marcel Dekker Inc., New York, 1998, vol. 35.
- 2 Iron Biominerals, ed. R. B. Frankel and R. P. Blakemore, Plenum Press, New York, 1989.
- 3 D. Gatteschi and R. Sessoli, *Angew. Chem. Int. Ed. Engl.*, 2003, **42**, 268 and references therein.
- 4 R. E. P. Winpenny, *Adv. Inorg. Chem.*, 2001, **52**, 1.
- 5 R. Laye and E. J. L. McInnes, *Eur. J. Inorg. Chem.*, 2004, 2811.
- 6 W. Schmitt, M. Murugesu, J. C. Goodwin, J. P. Hill, A. Mandel, R. Bhalla, C. E. Anson, S. L. Heath and A. K. Powell, *Polyhedron*, 2001, **20**, 1687.
- 7 W. Schmitt, C. E. Anson, B. Pilawa and A. K. Powell, *Z. Anorg. Allg. Chem.*, 2002, **628**, 2443.
- 8 W. Schmitt, E. Baissa, A. Mandel, C. E. Anson and A. K. Powell, *Angew. Chem. Int. Ed. Engl.*, 2001, **40**, 3577.
- 9 S. L. Heath, P. A. Jordan, I. D. Johnson, G. R. Moore, A. K. Powell and M. Hellwell, *J. Inorg. Biochem.*, 1995, **59**, 785.
- 10 A. K. Powell, S. L. Heath, D. Gatteschi, L. Pardi, R. Sessoli, G. Spina, F. Del Giallo and F. Pieralli, *J. Am. Chem. Soc.*, 1995, **117**, 2491.
- 11 See for example: F. A. Cotton and G. Wilkinson, *Advanced Inorganic Chemistry*, Wiley-Interscience, New York, 4th edn., 1980, p 758.
- 12 R. M. Cornell and U. Schwertmann, *The Iron Oxides*, VCH, Weinheim, 1996.
- 13 A. Herpin, *Theorie du Magnétisme*, *Bibl. des Sciences et Techn. Nucl.*, Presses de France, 1968.